New Composite Nighttime Light Index (NCNTL): A New Index for Urbanization Evaluation Research

Haofan Ran ⬤, Fei Zhang ⬤, Ngai Weng Chan ⬤, Mou Leong Tan ⬤, Hsiang-Te Kung, and Jingchao Shi

Abstract—This article employs the 2018 National Polar-Orbiting Partnership/Visible Infrared Imaging Radiometer Suite (NPP/VIIRS) and Luojia_01 nighttime light imagery to construct a New Composite Nighttime Light Index, which is NCNTL. The reliability of NCNTL is verified based on the analysis of urban road network, population, and Landsat normalized difference vegetation index auxiliary data. The research found some differences between the NPP/VIIRS and the Luojia_01 nighttime light imagery in detecting urban areas by comparing and analyzing the urban area factor of the Xinjiang region. Therefore, NCNTL was developed to solve this issue. First, a more significant improvement of correlation was found between NCNTL and the city-related factors than that in a single nighttime light imagery source. Second, the conformation of the NCNTL integration of the characteristics of multisource nighttime light was achieved to a certain extent by using NPP/VIIRS and Luojia_01 to extract urban area features. Third, NCNTL outperformed the single-source data in extracting small- and medium-sized cities in southern Xinjiang. With the application of the new nighttime index, researchers can now fuse nighttime light imagery easily to perform urban analysis. Although the quality of NCNTL is similar to nighttime light imagery processed using multisource auxiliary data, it can greatly reduce the workload in urban analysis and decrease the complex task requirement of collecting data from multiple sources.

Index Terms—Luojia_01, National Polar-Orbiting Partnership/Visible Infrared Imaging Radiometer Suite (NPP/VIIRS), urbanization.

I. INTRODUCTION

CITIES have evolved into a major habitation area for the world's population and have become the main carrier object of social civilization and economic growth in the 21st century [1], [2]. Based on the background of urbanization, nighttime light has become a reliable data source and has been gradually introduced into the analysis or evaluation of urbanization and various human activities [3], [4]. In the past, nighttime light was mostly studied based on Defense Meteorological Satellite Program/Operational Linescan System (DMSP/OLS) nighttime light data for urban spatial land distribution analysis, population density simulation, economic level evaluation, urban development model evaluation, etc. However, due to the lack of on-board calibration or continuous calibration, the data quality was poor, and there were many problems such as data saturation and blooming, and lack of ability to extract details from the inner city [5], [6], [7]. As the data resolution is about 1 km, it cannot depict much details of urbanization within a city. Similarly, the National Polar-Orbiting Partnership/Visible Infrared Imaging Radiometer Suite (NPP/VIIRS) data with 500 m resolution, which is mostly used for population estimation and gross domestic product (GDP) gridding, has the problem of background noise [6], [8], [9]. Luojia_01, the world's first professional night light remote sensing satellite, was launched in June 2018. With the spatial resolution reaching 130 m and the required time being significantly reduced, the global nighttime light imaging can be completed within 15 days [10], [11]. As such, the Luojia_01 with high resolution can provide a more accurate data reference, which is highly dependable on China's regional economic modeling, urban development, and change analysis. It has significant application values for the studies of social and economic environment [11], [12], [13]. According to the existing research, the nighttime light image of the Luojia_01 has great potential for studying the level of urbanization and the simulation of social and economic statistics, which can be used as a more reliable data source for the establishment of social and economic indicators [14], [15]. For example, the Luojia_01 nighttime light imagery was used to effectively identify a city's market and to explore the trend of urbanization [13]. In addition, there is a huge potential in the joint application of the Luojia_01 nighttime light imagery with big data in terms of analyzing the supply and demand of urban land as it can effectively respond to an urban land at the level of urbanization [16], [17].

Scholars in China and other countries have also done a lot of research on how to use nighttime light data to reflect the internal details of cities and to solve the blooming of nighttime light data problem [10]. To solve this problem, there are three main methods: desaturation method based on the frequency distribution of light DN value [18], desaturation method based on invariant target area [19], [20], [21], and desaturation method that based on auxiliary parameters of city correlation factor [22], [23], [24], [25], [26], [27], [28], [29], [30]. Although the first

Haofan Ran is with the University of Chinese Academy of Sciences, Beijing 101408, China (e-mail: ranhaofan@126.com).

Fei Zhang is with the College of Geography and Environmental Sciences, Zhejiang Normal University, Jinhua 321004, China (e-mail: zhangfei3s@163.com).

Ngai Weng Chan and Mou Leong Tan are with the GeoInformatic Unit, Geography Section, School of Humanities, Universiti Sains Malaysia, Penang 11800, Malaysia (e-mail: nwchan1@gmail.com; mouleong@usm.my).

Hsiang-Te Kung and Jingchao Shi are with the Department of Earth Sciences, University of Memphis, Memphis, TN 38152 USA (e-mail: hkung@memphis.edu; jshi@memphis.edu).
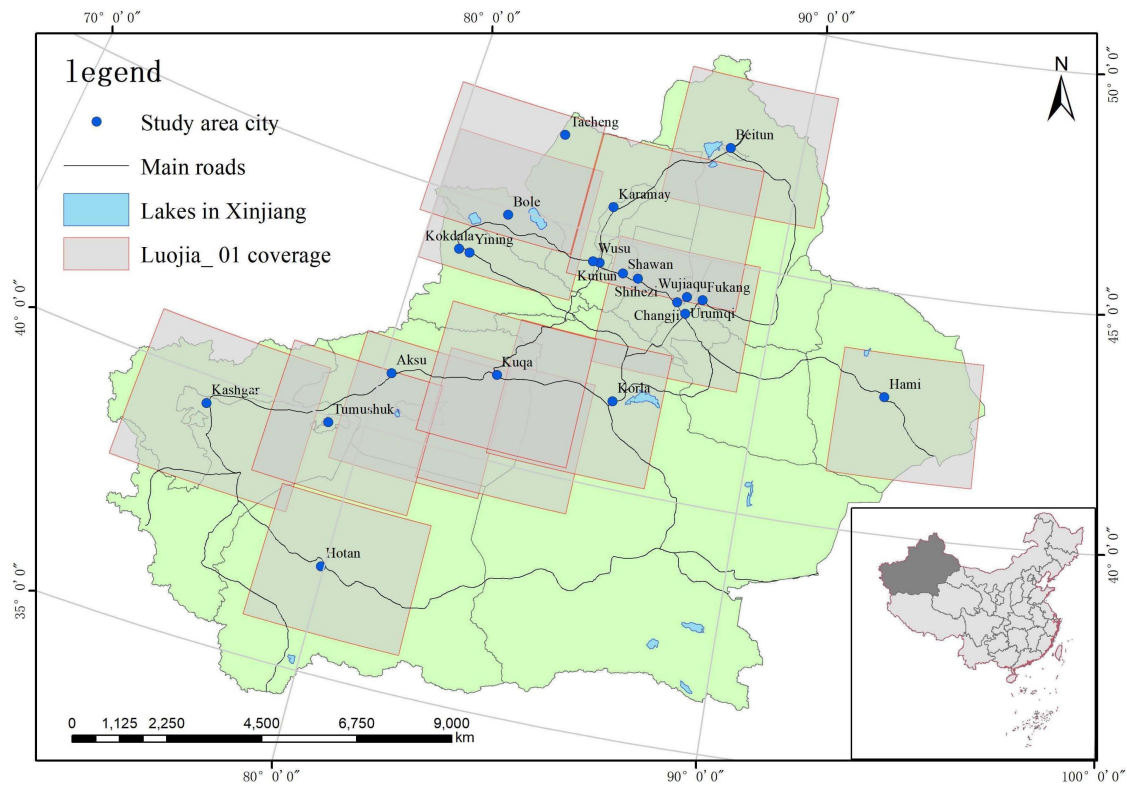
Fig. 1. Location map of a study area.

two methods are mainly employed to solve the nighttime light saturation phenomenon in DMSP/OLS, the third method is more widely used. Among the three, there are mainly modified light indices that are based on normalized difference vegetation index (NDVI) and enhanced vegetation index (EVI). But these methods usually lead to errors since single vegetation index correction is not significant enough, with the corrected nighttime light index losing a part of the information carried by the data itself [31]. Therefore, it is essential to improve the nighttime light index to make it more consistent with the progress of urbanization in terms of data resolution and quality. Furthermore, research on the correction of the nighttime light index is mostly conducted based on DMSP/OLS or NPP/VIIRS data. Finding a way to quickly correct the nighttime light index combined with new high-resolution light data is very important to solve the law of human surface activities more closely [32], [33].

Given this background, the basis of this study uses the Luojia_01 and NPP/VIIRS nighttime light imagery combined with relevant city data to develop a New Composite Nighttime Light Index (NCNTL). Therefore, the aims of this study are as follows.

1) To evaluate the efficiency of NCNTL in specific urban areas and single lighting.
2) To assess the detailed differences of the NCNTL with the Luojia_01 and the NPP/VIIRS light index in city regions.
3) To analyze the correlation between NCNTL in urban areas with single nighttime light imagery, population, street network, vegetation, and other factors change.

4) To use the threshold extraction method of NCNTL to extract the built-up area, and then compare with SVM-based regional self-growth algorithm that uses NPP/VIIRS, NDVI, and Luojia_01 as data source.

Finally, the reliability of NCNTL in urbanization analysis was evaluated. NCNTL helps to decrease the complexity of data collection to a certain extent and concise the data preprocessing and preparation work in urban studies.

A. Data Sources and Preprocessing

The research target of this study is the cities in Xinjiang Uygur Autonomous Region of China. Xinjiang is extremely rich in natural resources and historical culture, covering an area of approximately 1.66 million km^2. The research range is between longitudes 73°E to 97°E and latitudes 35°N to 50°N (see Fig. 1). Since the beginning of the 21st century, the economy of Xinjiang has grown rapidly, and the urban area has expanded greatly in recent decades. According to incomplete statistics, the urbanization level of Xinjiang's population has grown at a fast rate, exceeding 40% in 2010. The towns in southern Xinjiang increased by 41.39% year-on-year in 2000, and the overall growth rate was 34.80% year-on-year [34], [35]; during this period, the urbanization in the north and south of Xinjiang accelerated significantly, and the urban agglomeration on the northern slope of the Tianshan Mountains is widely researched as an academic hotspot [36], [37]. Therefore, this study focuses on the current status of Xinjiang's urbanization with major cities

TABLE I
BASIC DATA SOURCES INFORMATION IN THE STUDY

Data name	Date type	Resolution (m)	Data time range (year)	Data link	Data introduction
NPP/VIIRS	Raster	740	2018-08-01–2018-12-01	https://ladsweb.modaps.eosdis.nasa.gov/search/order/1/VNP46A1--5000	Data are extremely rich (some monthly average images and daily images can be downloaded for free)
Luojia_01	Raster	130	2018-08-01–2019-08-23	http://59.175.109.173:8888/app/login.html	5772 images Available for free download
EULUC-China	Vector	-	2018	http://data.ess.tsinghua.edu.cn/	Free access
WorldPOP	Raster	100	2018	https://www.worldpop.org/geodata/summary?id=6026	free access, rich data sources, based on annual update
OSM-OpenStreetMap	Vector	-	2018	https://www.openstreetmap.org/#map=4/36.96/104.17	Large amount of data and clear data hierarchy
Landsat-8	Raster	30	2018-06-01–2019-08-01	https://www.usgs.gov/core-science-systems/nli/Landsat	Free access

as the object. Urbanization plays an extremely important role in portraying the economic level and social production capacity of Xinjiang. In addition, the study of urbanization has an important auxiliary function in Xinjiang's economic policy formulation and macrodevelopment strategy, laying the foundation for the long-term stable development of Xinjiang.

As shown in Fig. 1, this study mainly uses NPP/VIIRS of 2018 and Luojia_01 nighttime light imagery as the main data source and was supplemented by auxiliary data such as Landsat 7, OpenStreetMap (OSM), and world-POP data. Fig. 1 shows the main city area in Xinjiang covered by Luojia_01 in gray color. The auxiliary data essential urban land use categories in China (EULUC-China) were obtained from Gong et al. [16], which is mainly used for urban internal space segmentation, functional area comparative analysis, and built-up area classification accuracy evaluation. The data are only available for 2018 and are complex to produce, making it difficult to expand to other years for city study. Population data and road network data are employed to measure the level of urbanization and to extract the urban built-up area, whereas Landsat data are used to extract NDVI data of the area.

The data source is shown in Table I. The basic city statistical data involved in the study are from *Xinjiang Statistical Yearbook* and *China City Statistical Yearbook*. The vector data are from the *basic vector data of China's prefecture level cities in 2015* from the resource at environment data center of the Chinese Academy of Sciences. In data preprocessing, Loujia_01 and Landsat-8 are completed based on the Google Earth Engine (GEE) platform. The subsequent processing and algorithm are based on a Python environment, mainly by using the Arcpy package in ArcGIS to complete the batch processing of data.

B. Data Preprocessing

In this article, Luojia_01 nighttime light imagery is used for radiometric correction and NPP/VIIRS for outlier processing. Water mask removal is used to get land surface area. In addition,
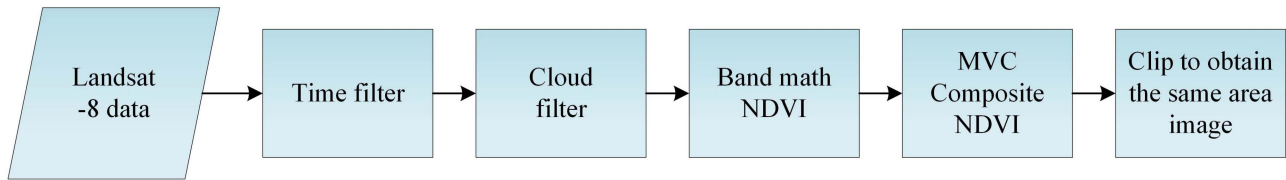
Fig. 2. Landsat-8 data extraction NDVI process.

Landsat-8 is used to extract NDVI, and OSM data are used to create road network levels.

In order to compare NCNTL with other nighttime light indices, we analyzed the two most common NDVI-based corrected nighttime light indices: EVI adjusted nighttime light index (EANTLI) [23] and vegetation adjusted NTL urban index (VANUI) [24]. Both indices are based on the basic understanding that urban surfaces and vegetation exhibit a negative correlation. The calculation equations are shown as follows:

$$\text{VANUI} = (1 - \text{NDVI}) + \text{NTL} \tag{1}$$

where NDVI values to the range of nonnegative values between 0 and 1.0. NTL is night light data

$$\text{EANTLI} = \frac{1 + (\text{NTL}_{\text{nom}} - \text{EVI})}{1 - (\text{NTL}_{\text{nom}} - \text{EVI})} \times \text{NTL} \tag{2}$$

where NTL_{nom} is the normalized NTL.

1) NPP/VIIRS Data Processing: There is a phenomenon of extremely bright values existing in NPP/VIIRS data, where only monthly data are presented but not interannual data. Therefore, it is necessary to fuse monthly data and eliminate outliers. Denoising processing is based on the idea of the literature [38]. The partial data using the GEE platform are obtained through continuous radiation correction and correction NPP/VIIRS data. The city that uses the center of region extremum DN value as a threshold eliminates abnormal pixel.

2) Extraction NDVI Based on Landsat-8 Data: As shown in Fig. 2, ee.ImageCollection ("Landsat/LC08/C01/T1_RT") is used to filter the data on the GEE platform, which is based on the Landsat-8 data. The data range is limited from 2018-06-01 to 2018-12-01. From nearly 400 images, the required data are filtered according to the cloud amount. The cloud amount is sorted from small to large, and the cloud content screening part is mainly based on the original image, which is derived by the ee.Algorithms.Landsat.simpleCloudScore function in the GEE platform. The NDVI index is calculated based on the ee.normalizedDifference function, and so is further data processing such as splicing, mosaic, and then cropping is performed. Finally, NDVI is synthesized according to the maximum value synthesis (MVC) algorithm [39].

The NDVI algorithm formula is shown as follows:

$$\text{NDVI} = (\rho_{\text{NIR}} - \rho_{\text{NR}})/(\rho_{\text{NIR}} + \rho_{\text{NR}}) \tag{3}$$

where ρ_{NIR} is the reflection value of Landast-8 data in the near-infrared band, and ρ_{NR} is the reflection value of the red band.

The MVC algorithm was proposed by Holben [39] in 1986 and is currently the most widely used vegetation index synthesis

algorithm

$$\text{NDVI}_{\text{mvc}} = \max[DN_i] \tag{4}$$

where DN_i is the maximum value of images in multiple periods. The maximum value is selected as the input of the DN value of the image, and the final output is the NDVI image of the region.

3) OpenStreetMap: The OSM project was created by a user community of geocoding datasets, which is an open-source geographic information data project dedicated to the production of infrastructure resources [40]. The structure of the dataset consists of the relationship between nodes and roads (open or closed, and area). The dataset can be used on multiple platforms as well. The file data are downloaded from this website (https://download.geofabrik.de/asia-latest.osm.pdf). The street data of road information in the dataset were served as the basic dataset. The specific operation process is shown as follows.

1) When the vector line data are selected, the original OSM data need to be decompressed and cropped in the Java Environment. The*. OSM data can be opened and exported in the open-source QGIS software.
2) Reclassifying the road network data is done according to the road grade.
3) The 3*3 sliding window calculates the sum of the pixels in its neighborhood as the cumulative level data of the road network.

4) Luojia Data Processing: Radiation correction is carried out for the Luojia_01 nighttime light imagery, and the pixel DN value is transformed into product radiation brightness. The specific formula is shown as follows:

$$L = DN^{3/2} \cdot 10^{-10}. \tag{5}$$

II. RESEARCH PROCESS AND METHODS

A. Technical Process

Details of the technical route are shown in Fig. 3. First, we select the central point of the major cities in Xinjiang as the regional center. Then, the center point is selected with a radius of 20–30 km, and this range is used as the study center of each city. The NPP/VIIRS and Luojia_01 are used based on the threshold of the maximum value of the center of each city to exclude the high-value image elements in the surrounding areas of the city. The specific processing of the NPP/VIIRS, Luojia_01, Landsat, OSM, and World-pop data is described in Fig. 3. After being processed, the data were used the nearest neighbor approach to resample to 500 m and then resample to 130 m using cubic convolution approach.
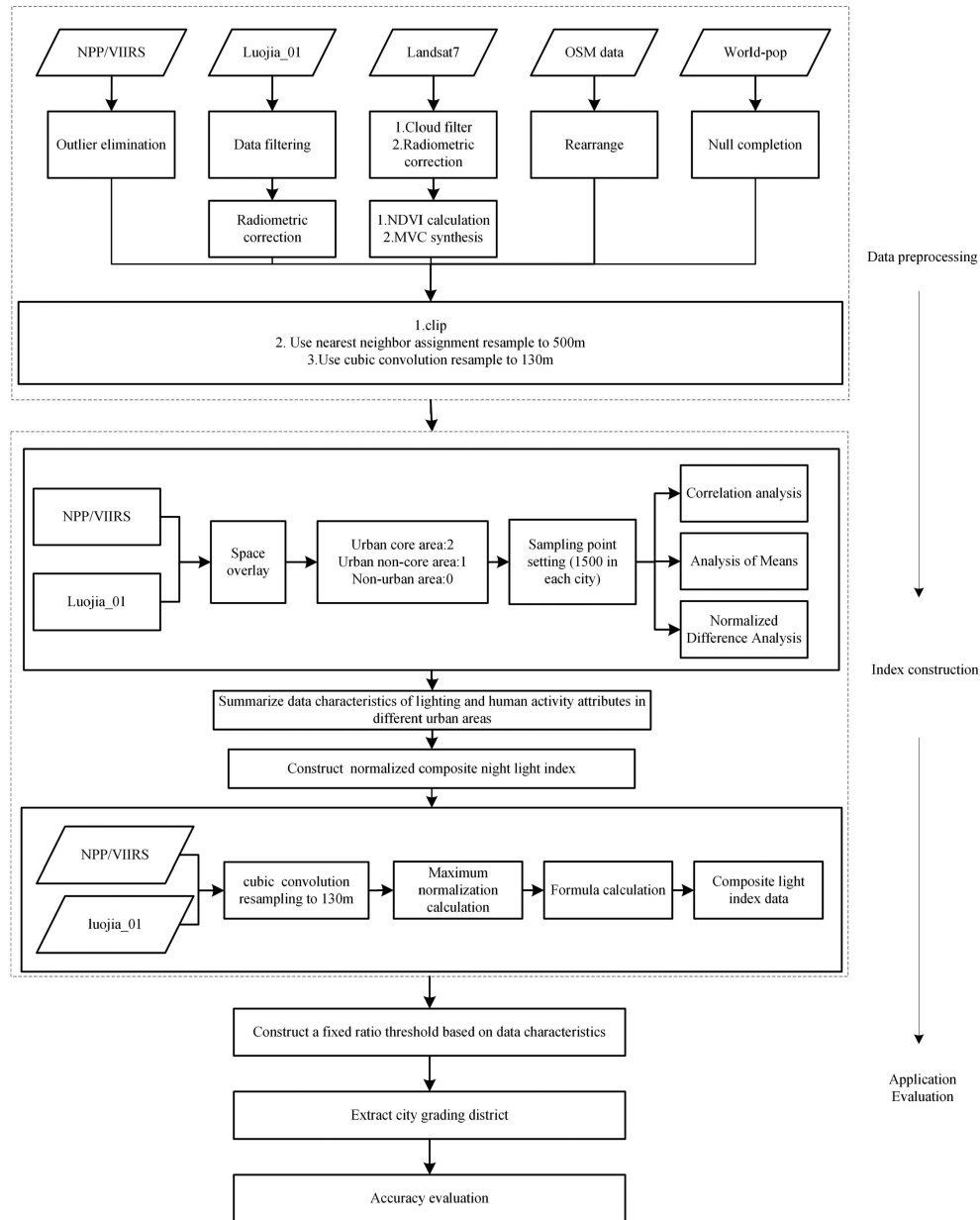
Fig. 3.   Technical flowchart.

This index formula (6) is not obtained from the beginning to analyze and compare the pattern between data. First, by the known city range, this datum is obtained from EULUC-China to distinguish the urban and nonurban areas and then correlate the lights and other geographic elements of the urban area to find the distribution pattern of the mean value as well as the distribution characteristics of the normalized data. Finally, the NCNTL equation is summarized. Then based on Luojia_01 and NPP/VIIRS, we used the SVM-based regional self-growth algorithm by Cao et al. [41] to extract the built-up areas of Xinjiang's main cities. A total of 1500 sampling points were set up for each city for analysis and comparison. Through the sampling analysis and comparison of urban-related factors, the data rules of urban and nonurban areas are explored. Based on this, the NCNTL can

be designed and constructed. Then, the NCNTL is evaluated and analyzed by methods such as correlation, urban light profile, and built-up area extraction applications.

B. Index Building Method

With the sampling points all set up, the normalized value law statistics of NPP/VIIRS and Luojia_01 nighttime light imagery for different urban core areas, urban noncore areas, and nonurban areas are shown in Fig. 4.

Fig. 4 shows the normalized mean values of nighttime lights in different regions and different cities. This result can be used to illustrate the characteristics of the urbanization level of major cities in Xinjiang. It can also be used to analyze the law of
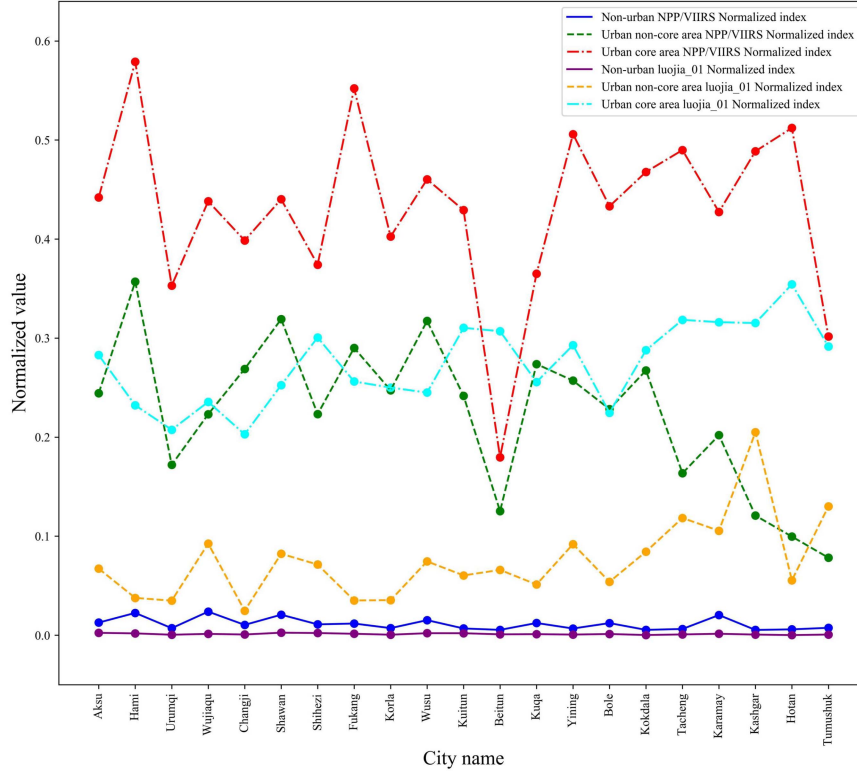
Fig. 4. NPP/VIIRS and Luojia_01 nighttime light imagery normalized urban grading mean map of major cities in Xinjiang.
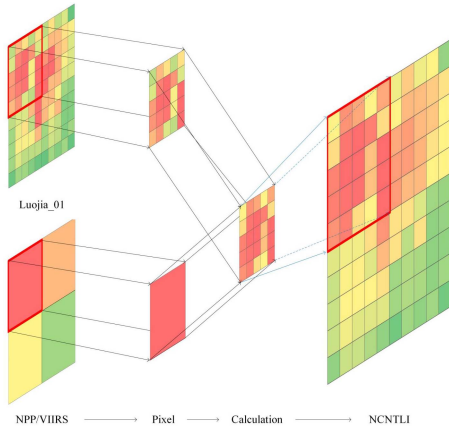

Fig. 5. Algorithm diagram.

differentiation of nighttime lights in the interior of the city. In addition, NPP/VIIRS and Luojia_01 all reflected the data values of core to the nonurban area gradually decreasing. These constitute an obvious proportional relationship. Moreover, the two datasets are in the core and noncore urban areas of the city, showing a high degree of consistency and the same data distribution trend. However, the relationship between the two datasets is different. The two trends are consistent, but there are differences in the normalized values. In nonurban areas, the data are basically close to 0, indicating that there is little difference in the data in this area. In summary, this difference comes from the characteristics

of different light data collection and sensor characteristics. This regular distribution difference shows nighttime light imagery of different scales from different sources. Finding the way to combine the characteristics between the two data is the key to constructing NCNTL. Therefore, based on the characteristics of this datum and combining the differences between the two datasets, this article proposes NCNTL, with the formula shown as follows:

$$NCNTL = npp \times (1 + (luojia_{nom} - npp_{nom})/(luojia_{nom} + npp_{nom})) \tag{6}$$

where npp is the NPP/VIIRS data, $luojia_{nom}$ is the Luojia normalized by the maximum value data, and npp_{nom} is the light data normalized by the maximum value.

The DN of any position of the image in the Luojia_01 is D_1; the normalized maximum interval is a constant N; the DN of pixels at the same position in the NPP/VIIRS is D_2; and the normalized interval length is a constant M. So, we have the following expression:

$$NCNTL = npp \times \left(\frac{ND_1 - MD_2}{ND_1 + MD_2} + 1 \right). \tag{7}$$

And then, the transformation of (7) leads to

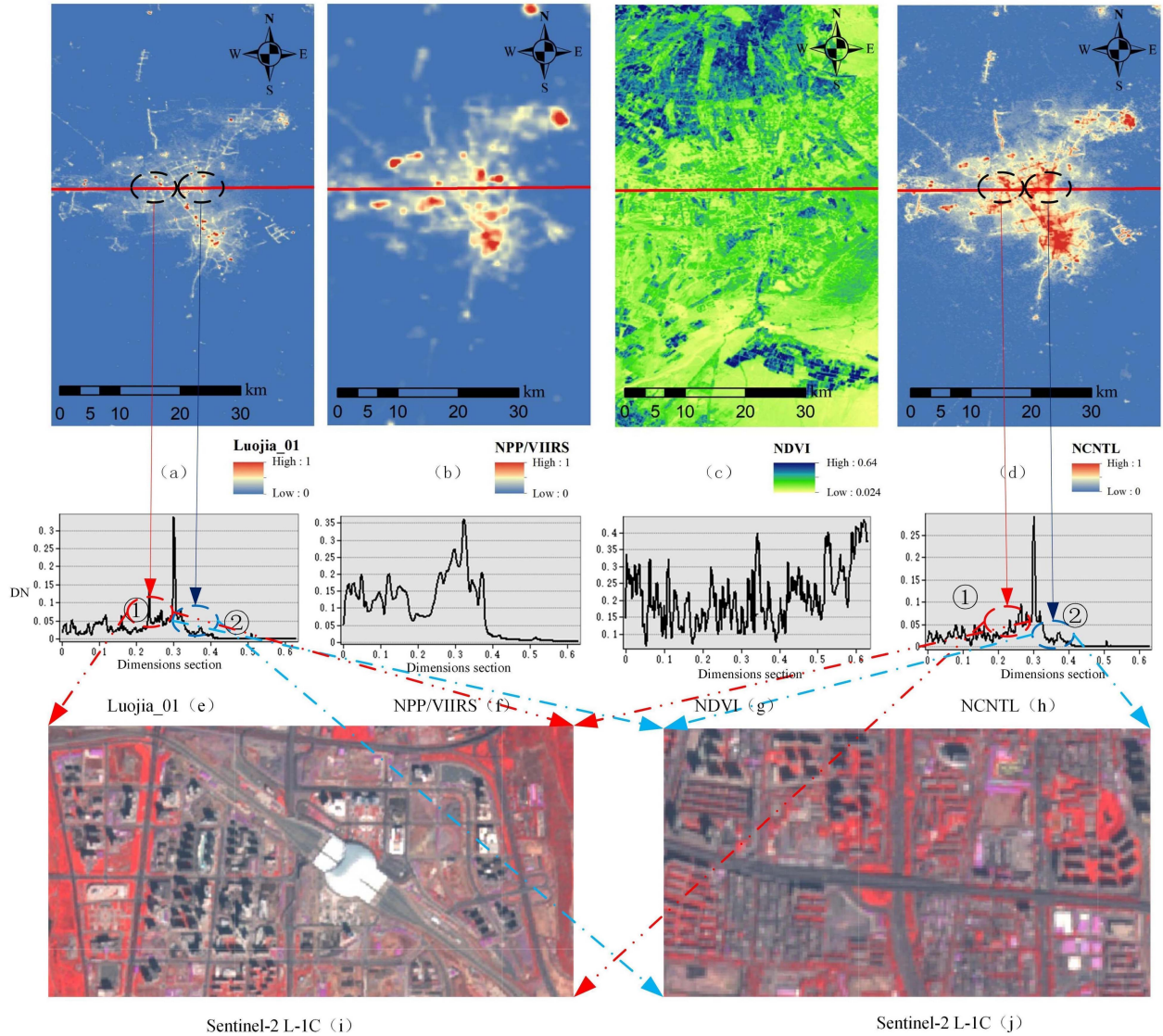$$NCNTL = npp \times \left(\frac{2ND_1}{ND_1 + MD_2} \right). \tag{8}$$
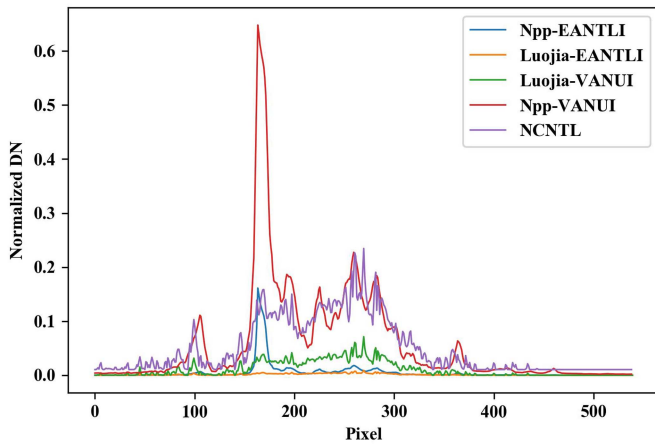
Fig. 6. Urumqi lighting data profile.

Fig. 7. Latitudinal transects of the normalized NPP/VIIRS EANTLI, Luojia_01 EANTLI, Luojia_01 VANUI, NPP/VIIRS VANUI, and NCNTL along one dimension transect in Urumqi.

We define the adjustment factor k in (8) as

$$K(D_1, D_2) = \frac{2ND_1}{ND_1 + MD_2}. \qquad (9)$$

Then, we can conclude (10) and (11)

$$K(D_1, D_2) > 0 \qquad (10)$$

$$\frac{\partial [K(D_1, D_2)]}{\partial (D_1)} = \frac{2MND_2}{(ND_1 + ND_2)^2}. \qquad (11)$$

So NCNTL can be written as

$$\text{NCNTL} = K \times npp. \qquad (12)$$

Here, it is known in formula (10) that K is greater than 0. A single-tuning function of D_2 and D_1 can be obtained by the deflection number of the K for D_1, which is greater than zero when the function is greater than zero. Therefore, the change
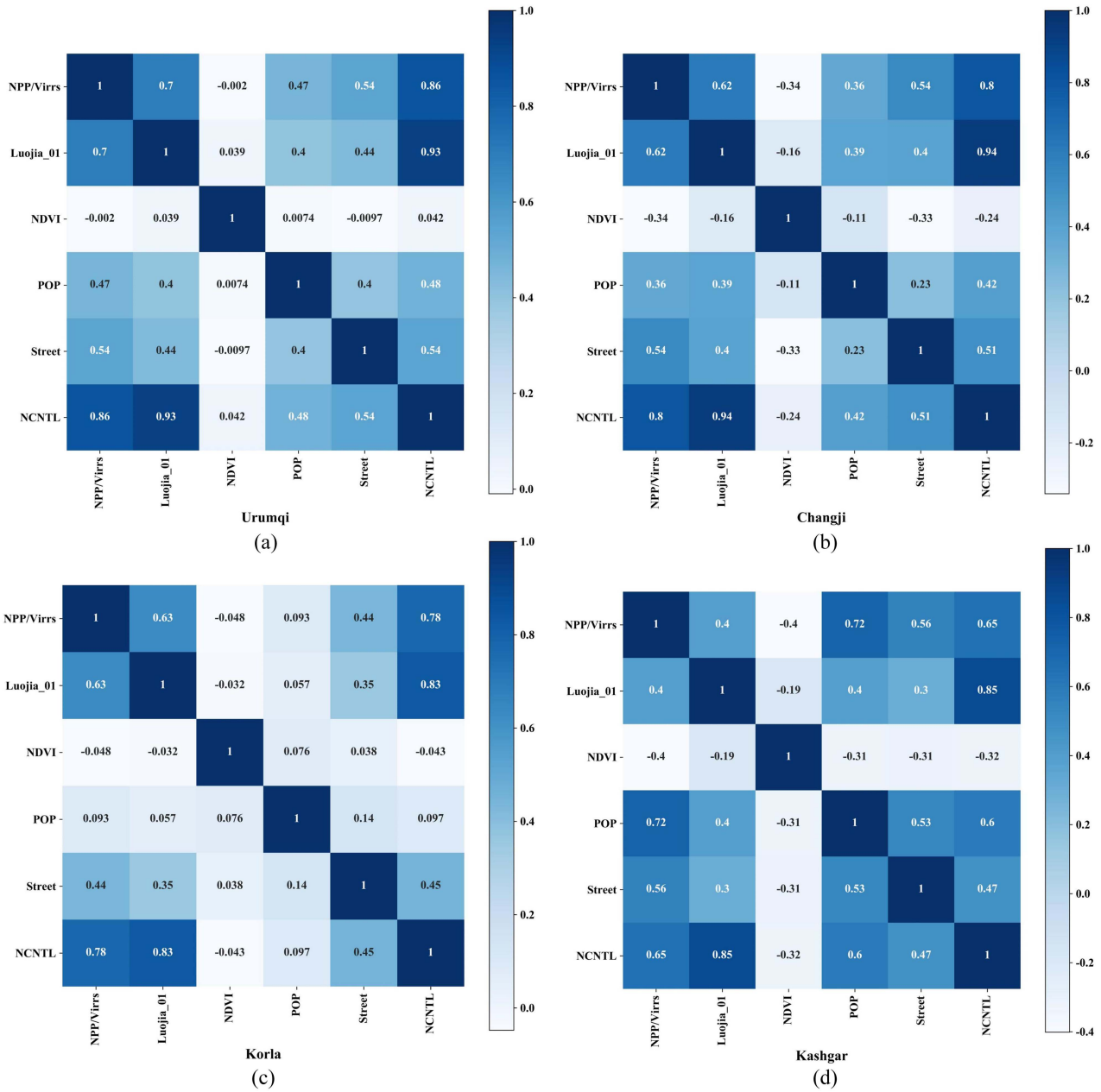
Fig. 8. Correlation coefficient matrix of composite lighting data and related city data factors.

in K is related to the variation of the two image elements, and NCNTL is changed by the Luojia_01 and NPP/VIIRS.

Fig. 5 shows there is spatial variability between NPP/VIIRS and Luojia_01. High-value image areas of NPP/VIIRS are not necessarily to represent the real surface bright images. In the same place, the NPP/VIIRS detected a higher value than NPP/VIIRS. The recently launched sensor has a high resolution, but its detected value may be lower than that of the same place under the NPP/VIIRS satellite. Hence, the combination of high and low spatial resolution lighting data can enrich the variation in unit pixel, which is the advantage of this multisource lighting index. It should also be applied to other kinds of nighttime light data.

III. RESULTS AND ANALYSIS

A. Benefits of Evaluation of New Compound Light Index in Urban Area

In order to evaluate the detailed characteristics of the new composite light index (NCNTL) compared with a single index (Luojia_01, NPP/VIIRS, and NDVI) in the city more intuitively, this article selects Northern Urumqi light profiles as the analysis objects, and the results are shown in Fig. 6.

Vertical coordinates in Fig. 6(e)–(h) are the normalized DN values, and the horizontal coordinates are the relative proportions of the widths of the (a)–(d) plots. All the (a)–(d) plots used Gaussian linear 2% stretching with 130 m resolution for
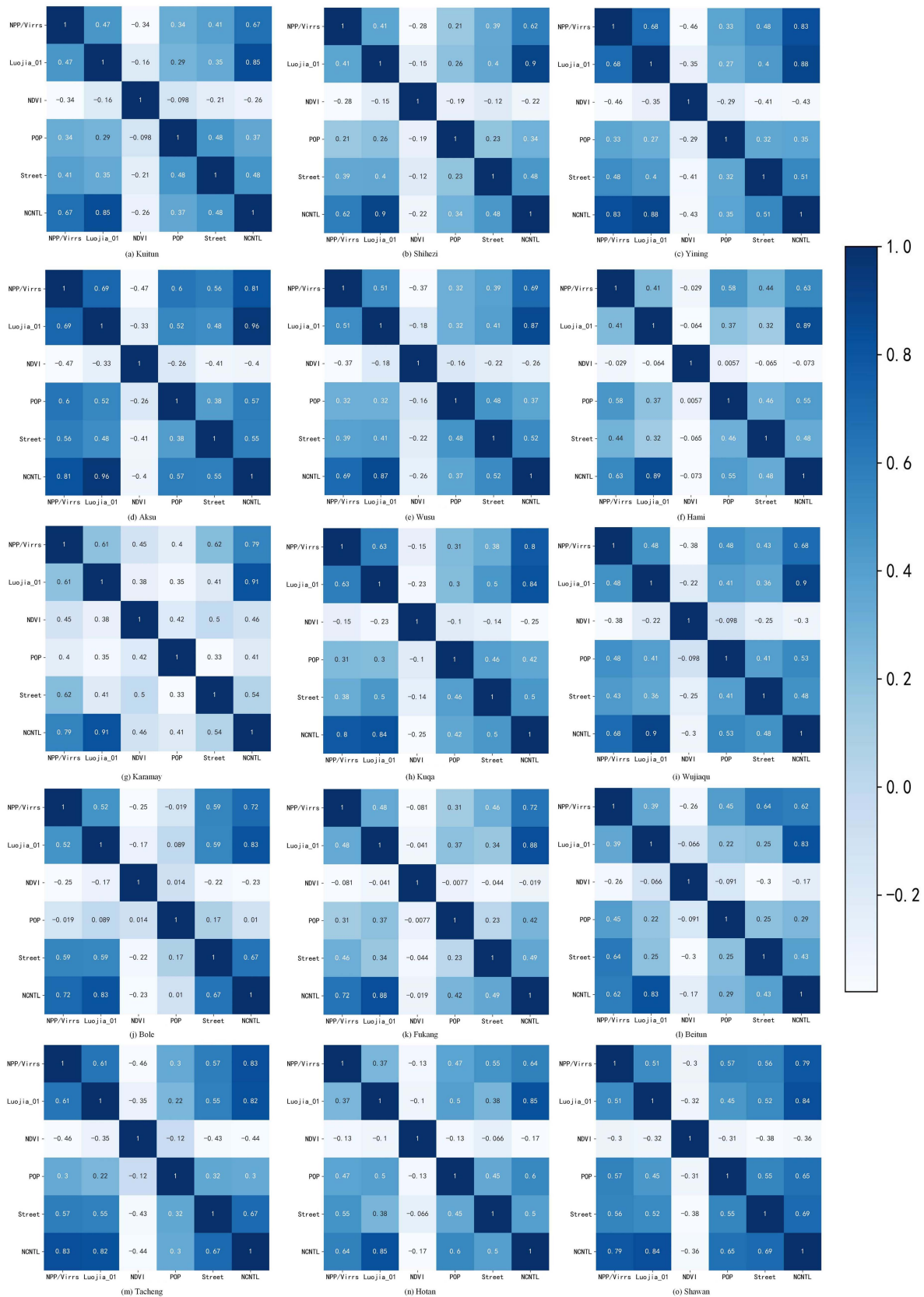
Fig. 9. Correlation coefficient matrix of NCNTL and related city data factor.
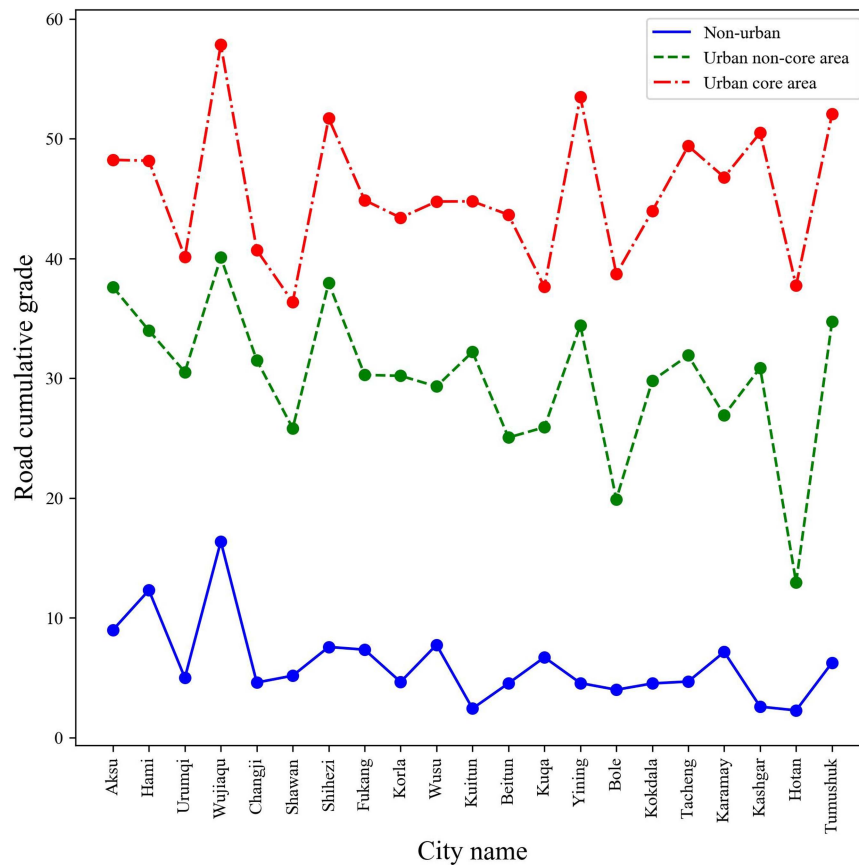
Fig. 10. Comparison of cumulative grades of roads in major cities in Xinjiang.

comparison, where (a) and (b) are normalized images. Fig. 6 shows that for area ①, the extremely high value is suppressed in the high-resolution Luojia_01 data. The detailed information around the extremely high value in imagery is supplemented by NCNTL. This part of the area is a residential area, and the high value next to it is the high-speed railway station. The high value may be caused by the side of the railway lighting lamp. The details of the NPP/VIIRS data have been effectively improved, and the rising trend of its light value has been retained, which is in line with the distribution of buildings on the ground. In area ②, it can be seen from the high-score image that this place is elevated, and the surrounding area is densely populated. The different feature of this part is added to the new conforming light index, and the data feature of NPP/VIIRS is retained.

In general, the new composite light index offers the possibility of improving the spatial resolution of large-scale low-resolution light images. Second, the urban interior details are added to suppress the abnormal values caused by unstable light sources in high-resolution lighting. So, to some extent it can avoid the relative radiometric correction process of immature lighting products. Third, the light data are fused at the pixel level, which retains the characteristics of the two. According to the difference between the long time series stable nighttime light products and the short time series instantaneous nighttime light images, the feature extraction and feature superposition are carried out; this result shows the increase in the city interior

details of NPP/VIIRS light data and suppresses the Luojia_01 data detail noise and slows down the overflow effect of light data. In nonurban areas, the light value is lower without using the NDVI and LAI, enabling it to better meet the scene analysis and comparison of urban nighttime light modeling in arid and semiarid areas with low vegetation cover.

This article calculated some other lighting indices, such as calculated EANTLI and VANUI based on NPP/VIIRS and NDVI; calculated EANTLI and VANUI based on Luojia_01 with NDVI. On this basis, one dimension of the city of Urumqi, which has the largest population in the study area, is chosen to bring a response to the differences among the indices. A possible explanation of the peak under NPP-VANUI is due to the extremely bright surface image grid, where the chosen transect has a stable light near to the station. Besides that, the Luojia_01 calculated index is lower than that of the NPP/VIIRS data because the transects area is not a real surface source location. It can be seen from Fig. 7 that the light indices that were generated based on NPP/VIIRS are all slightly smoothed, and Luojia_01 data are not suitable for the EANTLI in the Xinjiang area. Luojia_01 EANTLI has less variation in data on a certain dimensional band after normalization. This phenomenon also arises when using the Luojia_01 data to calculate the VANUI data. As it can be seen from the NCNTL, the data have significantly more variation detail, and more spatial variation can be seen by combining the change salient points of both Luojia_01 and NPP/VIIRS.
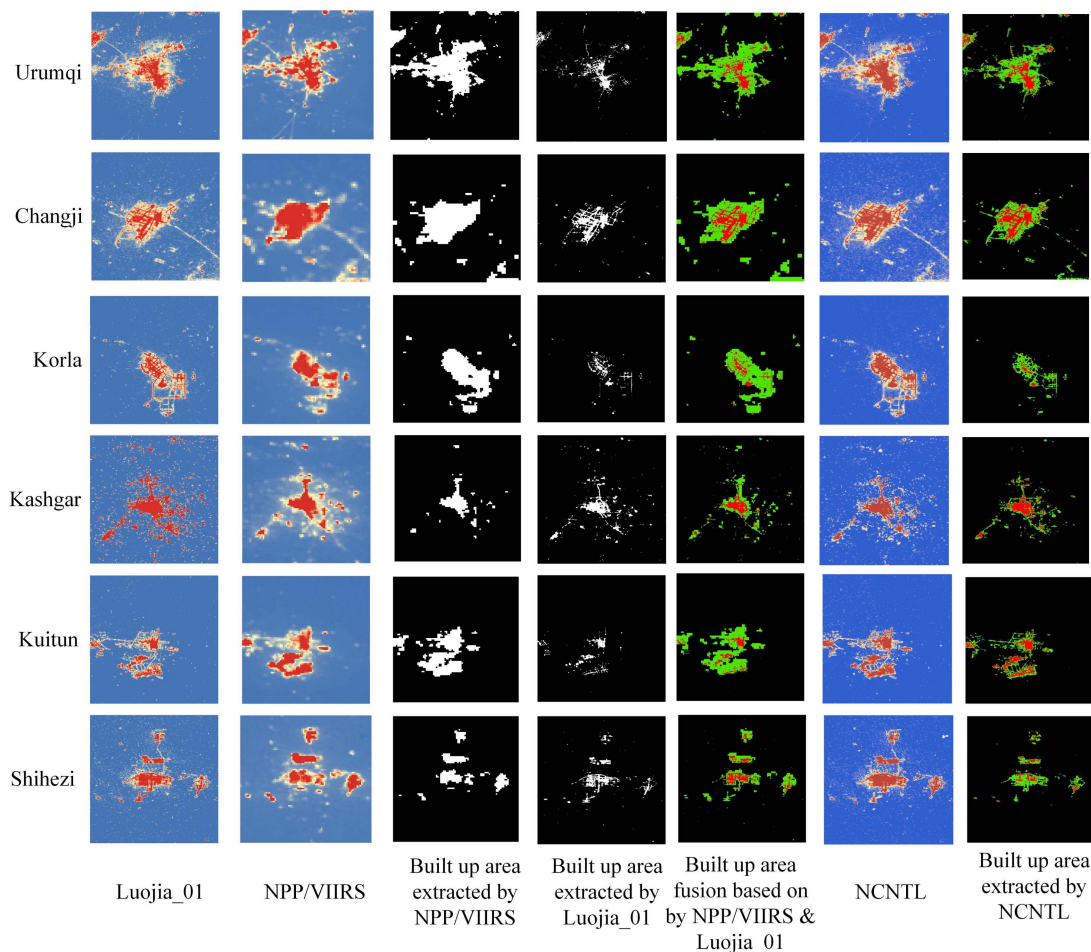
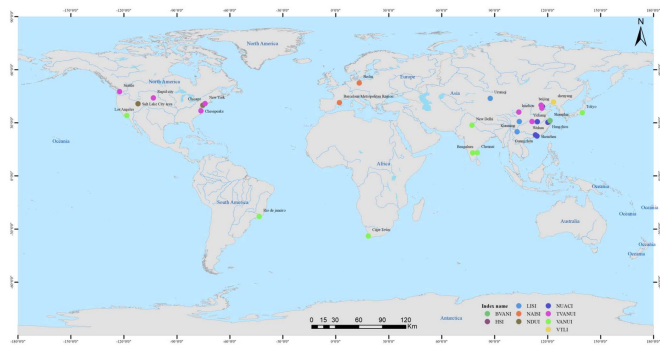Fig. 11.   NCNTL extraction built-up area classification map.

Fig. 12.   Nighttime light index study distribution.

B. Correlation Evaluation of New Composite Light Index

The correlation coefficient matrix of Urumqi, Changji, Korla, Kashi, etc., cities is selected. Different city factor attribute data were used to quantitatively compare and analyze the advantages of NCNTL and single light data source.

In Fig. 8, first, the Luojia_01 and the NPP/VIIRS nighttime light imagery show a high degree of correlation, and the NCNTL improves the correlation between the two nighttime light data. For example, the correlation between Luojia_01 and NPP/VIIRS data in Urumqi is 0.70, but the correlation between NCNTL and Luojia_01 has increased to 0.86 and 0.93, respectively; the correlation between Luojia_01 and NPP/VIIRS data in Changji is 0.62, but the correlation between NCNTL and Luojia_01 has increased to 0.80 and 0.94, respectively; the correlation between Urumqi's Luojia_01 and NPP/VIIRS data is 0.63, whereas the calculated correlation between NCNTL and Luojia_01 has increased to 0.78 and 0.83, respectively.

Fig. 9 shows other cities' correlation indices. The correlation indices of other cities also satisfy the above four city correlation variation characteristics. In the comparison of the correlation between the lighting data and the city-related factors, the correlation of the composite nighttime light Index is also better. Among all the research cities in Xinjiang, the correlation between NCNTL, population data, and road network-level data is significantly higher than that of single nighttime light data. Since Xinjiang is located in an arid and semiarid area, the negative correlation between the lights of major cities in

TABLE II
KAPPA COEFFICIENT OF EXTRACT BUILT-UP AREA

City name	Regional growth algorithm built-up area	NCNTL-proportion threshold built-up area
Urumqi	0.767004323	0.679340212
Changji	0.653243676	0.732114597
Korla	0.553112234	0.466865593
Kashgar	0.577490563	0.590880762
Kuitun	0.656638093	0.67965773
Shihezi	0.523521119	0.625468954
Yining	0.587814234	0.624953447
Aksu	0.525734057	0.605127313
Wusu	0.670190933	0.661105934
Hami	0.688409275	0.71432087
Karamay	0.448420352	0.553203151
Kuqa	0.569818567	0.682936247
Wujiaqu	0.642801176	0.715113408
Bole	0.620025579	0.707682822
Fukang	0.402875147	0.577476507
Beitun	0.530222007	0.448700738
Tacheng	0.670665975	0.798234476
Hotan	0.23893368	0.396795314
Shawan	0.623945979	0.739833949
Tumushuk	0.376634949	0.664418411
Kokdala	0.278251166	0.608737126

Xinjiang and NDVI data is not obvious. In the meantime, NDVI is related to some other cities factors. Therefore, NCNTL is more effective than the traditional vegetation index modified light index in the urbanization research of arid and semiarid areas. Most importantly, it could better reflect the real human-land relationship and social activities.

C. Evaluation of Built-Up Area Extraction Results

1) Built-Up Area Extraction: According to the SVM-based regional self-growth algorithm proposed by Cao et al. [41], Luojia_01 and NPP/VIIRS were used to extract the built-up areas of major cities in Xinjiang. According to the cumulative level of roads in different cities shown in Fig. 10, it is obvious that there are different road densities in different areas of the city.

Therefore, it can be calculated with the sampled road network data: the nonurban area has an average upper limit ratio value of 0.07, which is used as the separation value between the city and the nonurban area, and the lower limit ratio value of the urban core area at 0.16. This ratio is used as the threshold of the ratio between the city's noncore and the core area. The built-up area

and the inner grading area of the city are quickly extracted with the fixed ratio coefficient based on the composite light index. Through the simple character to extract the urban built-up area, then compare the influences with different data.

In Fig. 11, the first and second columns are the radiation-corrected images of Luojia_01, NPP/VIIRS, and the sixth column is the calculated NCNTL. The third and fourth columns are the built-up areas extracted by the SVM-based regional self-growth algorithm. The fifth column is obtained by superimposing the third and fourth columns, both of which indicate the areas as urban core areas marked in red, the rest in green, and nonurban areas in black. The last column is the urban area range obtained by simple threshold segmentation based on NCNTL. It can be seen from Fig. 11 that the fused NCNTL retains the advantages of Luojia_01 and NPP/VIIRS. After extracting the built-up area with a fixed ratio threshold, it was discovered that the extraction result was roughly similar to the built-up area extracted by the previous Luojia_01 and NPP/VIIRS. The detailed information at the city boundary was more abundant, and the effect of light blooming was greatly reduced. This shows that it extracts the city boundary features more accurately. From the comparison of the third and fifth columns in the figure, the

TABLE III
NIGHTTIME LIGHT INDEX STUDY INFORMATION

Research time	Index name	Data source	Applications	Public time	Reference
2000	HSI	DMSP/OLS MODIS NDVI	Human settlements place	2008	Lu *et al.* [22]
2006	VANUI	DMSP/OLS MODIS NDVI	Reduce saturation increase variation in nighttime luminosity	2013	Zhang *et al.* [23]
2012–2013	large-scale impervious surface index	NPP/VIIRS MODIS NDVI	Mapping Impervious Surface Distribution	2015	Guo *et al.* [25]
2000–2002 2006–2008	Normalized difference urban index	DMSP/OLS MODIS NDVI	Map the built-up area	2015	Zhang *et al.* [26]
2000 2005 2010	Normalized urban areas composite index	DMSP/OLS MODIS EVI MODIS NDWI	Mapping Impervious Surface Distribution	2015	Liu *et al.* [27]
2000	Vegetation temperature light index	DMSP/OLS MODIS NDVI	Reduce saturation Enhance Variation	2015	Hao *et al.* [28]
2010–2011	Temperature vegetation adjusted NTL urban index (TVANUI)	DMSP/OLS MODIS land surface temperature (LST) MODIS NDVI	Reduce saturation Enhance Variation	2018	Zhang Li *et al.* [29]
2013	Nighttime light adjusted impervious surface index	night-time color photographs from the International Space Station (ISS) Landsat	Mapping Impervious Surface Distribution	2019	Chen *et al.* [30]
2018	Building volume adjusted NTL index	Luojia_01 NPP/VIIRS	Population Distribution	2023	Wu *et al.* [33]

boundary between the urban intersecting area and the nonurban area is more refined, which is caused by the higher spatial resolution after the fusion of the two sets. Subsequently, based on the simple band calculation, threshold segmentation can get similar or even better results with a complex SVM-based area growth algorithm, which shows the superiority of this new type of composite light index.

2) Evaluation of the Extraction Accuracy of the Built-Up Area: In order to reflect the reliability of the built-up area extracted by the new light index, the kappa coefficient is used to evaluate the accuracy of the built-up area that is extracted based on the new light index.

The real surface classification data were obtained based on two steps: 1) the approximate classification data were first created in accordance with the built-up area defined by EULUC-China [16]; and 2) the preliminary identified points were compared with Landsat-8 for a finer classification. Finally, the extracted classified data are used to evaluate the regional classified built-up areas.

It can be seen from Table II that the built-up area extracted by the two methods has high accuracy and a high degree of consistency with the real classification data. However, the regional growth algorithm needs to use other auxiliary data

other than the construction area, and its iterative classification process is complex. The boundary of the built-up area extracted after using the normalized composite light index is closer to the real boundary. From a macroperspective, the jaggedness is weakened, the boundary is clear, and the impact of resolution is reduced. These characteristics are in part due to the input data difference. Second, among the 21 research objectives, the classification accuracy of 17 cities has been improved considerably. The highest accuracy increased by 118%, and the lowest increased by 2%. For all research objectives, the overall classification accuracy is increased by about 20.45%, which improves kappa (approximately 0.079) and has a significant effect on the extraction accuracy of the built-up areas. Among them, the extraction accuracy of built-up areas of small and medium-sized cities has been improved to a certain extent. The ranking order of built-up areas obtained from land-use data statistics is available. Among the research objects, the classification accuracy of the top ten cities with the built-up area has increased by about 3.4%, with the kappa coefficient increasing by 0.017. Also, the classification accuracy of subsequent urban built-up areas is increased by about 35.9%, with the kappa coefficient increasing by 0.135. From the view of the evaluation index of consistency of classification accuracy, the effect of normalized light index

TABLE IV
NIGHTTIME LIGHT SENSOR INFORMATION

Sensor	Spatial resolution (m)	Operational years	Temporal resolution	Products	Radiometric range	Spectral bands
Astronauts photographs onboard the ISS	5–200	From 2003 onwards (since mission ISS006)	Photographs taken irregularly	Photographs can be searched and downloaded from: http://eol.jsc.nasa.gov/	8–14 bit	RGB
Landsat 8	15–30	Launched in 2013	Photos taken irregularly	Freely available	14 bit Only very bright objects are detected	Seven bands
Jilin-1 (JL1-3B)	0.9	Launched in January 2017	Commercial satellite, acquires images on demand	Commercial	8 bit	430–512 nm (blue) 489–585 nm (green) 580–720 nm (red)
JL1-07/08	< 1	Launched in January 2018	Commercial satellite, acquires images on demand	Commercial	N\A	Panchromatic and multi spectral (blue, green, red, red edge, and near-infrared bands)
EROS-B	0.7	Night lights images offered since mid-2013	Commercial satellite, acquires images on demand	Commercial	16 bit	Panchromatic

extracting built-up area is significant, and the method is simpler. Researchers can obtain similar or even higher quality extraction results.

IV. DISCUSSION

Before this study, several scholars reconstructed urban spatial distribution details by using nighttime light imagery. For example, studies that are based on the light image element DN frequency distribution and constant target area [18], [32] by improving the observation accuracy of urban nighttime light imagery. At the same time, the surface vegetation index, or the temperature index, was also introduced to correct the urban nighttime light index, which can obtain better results [31], [32]. For example, human settlement index (HSI), VANUI, and EANTLI all reduce soil background interference to obtain better urban spatial light distribution [22], [23], [24]. In addition, there are GDP grid data and road network data to correct the data lighting in urban space [10], [43]. These can more accurately reflect the distribution details of lights inside the city. There is more nighttime light imagery available for researchers to choose from with more nighttime light sensors. On a secondary basis, obtaining urban nighttime spatial distribution through multisource light images becomes more imaginative.

In the construction and use of NCNTL, the difference in nighttime light remote sensing images of different sources was successfully corrected. Through sampling analysis, we confirmed that NCNTL is much more related to urban land and human data factors than single nighttime light imagery. The section analysis of the urban nighttime light index of NCNTL shows the difference and the details. In urban edge areas, the integration of image metadata data of different scales of data can be realized. Extraction of urban built-up areas using NCNTL confirmed that the method could retain urban spatial edge detail and that the point had greater extraction accuracy for the built-up area than a single data source. Meanwhile, the author selected cities of different climatic zones and socio-economic levels for extensive comparisons on a global scale or a national scale in China, as shown in Fig. 12.

The detailed related index research content in Fig. 12 is shown in Table III. The authors compared the indices constructed using nighttime light imagery. Previous studies have shown the reliability of the indices constructed using nighttime light imagery from different sources. Compared with Wu et al. [33], this study focuses on describing the use of NCNTL in mapping impervious surface distribution and increased variation in nighttime luminosity.

Furthermore, NCNTL is not limited to Luojia_01 versus NPP/VIIRS. It can communicate with night light data in two different spatial resolutions. As shown in the following table, the satellite data developed in recent years can replace Luojia_01 data, which refers to the work of Levin et al. [44], as shown in Table IV.

Despite these advantages, NCNTL still has limitations. First, NCNTL is limited to the data source and needs to be acquired within the same time domain range. Second, when one side data are of poor quality, the results are greatly affected. According to the correlation coefficient of NCNTL and NDVI in Changji, NCNTL is still affected by the correlation coefficient of Luojia_01 and NDVI, leading to a decrease in its correlation coefficient. This suggests that NCNTL is affected by one side value and loses a portion of the parameter properties associated with the land data during fusion. During fusion, correlation with road network data and NDVI data is based on neutralization. This feature indicates losses of the authenticity of a part of the data during the construction NCNTL process, and it cannot distinguish the image metadata with small differences. NCNTL needs further exploration of the advantages, disadvantages, and scope of application.

However, for specific urban refinement studies, NCNTL can still serve as a nighttime light index with a fusion of different scale characteristics to reflect the night condition of the city. NCNTL provides a simple way of light data fusion, a way of processing the nighttime light imagery in urban applications and reducing the workload and data search processing work. Through comprehensive analysis, such as urban expansion, temporal-spatial distribution of population, nighttime pollutant level, the temporal dynamics of socio-economic and demographic change status, etc., NCNTL could be better compared with a single light data. Conducting more three-dimensional analysis and tracking of urban centers could be realized.

V. CONCLUSION

In this article, Luojia_01 and NPP/VIIRS nighttime light imagery extraction range were employed to examine Xinjiang's built-up area of major cities. On this basis, NCNTL is proposed by fusing the multisource nighttime light imagery, and the reliability of its application is evaluated. The main conclusions include the following.

1) Construct NCNTL by using multisource data, such as NDVI, population, road network, etc., within the city to explore the data of city lights distribution characteristics.

2) Evaluate the reliability of NCNTL applications in the city and assess the correlation between the urban surface factors and human distribution.

3) Proved that NCNTL is reliable compared to single-source nighttime light imagery and various urban factors. By extracting urban building areas, the results show that the extraction accuracy of many cities in the south of Xinjiang has been significantly improved.

4) Provides a simple way to fuse nighttime light imagery, and the result can be comparable to World-pop, OSM, and other multisource data processed nighttime light imagery in urban applications, greatly reducing the workload.

Despite the promising results of this study, there are still some shortcomings and points that need to be addressed.

1) Since the study area in this study is focused on the arid and semiarid areas, the reliability of the NCNTL in other regions still needs further exploration and analysis.

2) This article only proposes a simple NCNTL, which is not significant at the low variance different nighttime light, and it will reduce the correlation with the NDVI-related factor. Therefore, the effectiveness of NCNTL still needs further research and improvement, especially in the application methods and design ideas.

REFERENCES

[1] United Nations, "World urbanization prospects: The 2014 revision, highlights," Department of Economic and Social Affairs, Population Division, United Nations, 2014.

[2] Z. Zhu et al., "Understanding an urbanizing planet: Strategic directions for remote sensing," *Remote Sens. Environ.*, vol. 228, pp. 164–182, 2019.

[3] Y. Ban, A. Jacob, and P. Gamba, "Spaceborne SAR data for global urban mapping at 30 m resolution using a robust urban extractor," *ISPRS J. Photogramm. Remote Sens.*, vol. 103, pp. 28–37, 2015.

[4] E. C. Stokes and K. C. Seto, "Characterizing urban infrastructural transitions for the sustainable development goals using multi-temporal land, population, and nighttime light data," *Remote Sens. Environ.*, vol. 234, 2019, Art. no. 111430.

[5] C. D. Elvidge, K. E. Baugh, J. B. Dietz, T. Bland, P. C. Sutton, and H. W. Kroehl, "Radiance calibration of DMSP-OLS low-light imaging data of human settlements," *Remote Sens. Environ.*, vol. 68, no. 1, pp. 77–88, 1999.

[6] M. M. Bennett and L. C. Smith, "Advances in using multitemporal nighttime lights satellite imagery to detect, estimate, and monitor socioeconomic dynamics," *Remote Sens. Environ.*, vol. 192, pp. 176–197, 2017.

[7] A. S. de Miguel, C. C. Kyba, J. Zamorano, J. Gallego, and K. J. Gaston, "The nature of the diffuse light near cities detected in nighttime satellite imagery," *Sci. Rep.*, vol. 10, no. 1, 2020, Art. no. 7829.

[8] L. B. Liao, S. Weiss, S. Mills, and B. Hauss, "Suomi NPP VIIRS day-night band on-orbit performance," *J. Geophys. Res., Atmos.*, vol. 118, no. 22, pp. 12705–12718, 2013.

[9] M. O. Román et al., "NASA's Black Marble nighttime lights product suite," *Remote Sens. Environ.*, vol. 210, pp. 113–143, 2018.

[10] W. Jiang et al., "Potentiality of using Luojia 1-01 nighttime light imagery to investigate artificial light pollution," *Sensors*, vol. 18, no. 9, 2018, Art. no. 2900.

[11] X. Li, L. Zhao, D. Li, and H. Xu, "Mapping urban extent using Luojia 1-01 nighttime light imagery," *Sensors*, vol. 18, no. 11, 2018, Art. no. 3665.

[12] X. Li, X. Li, D. Li, X. He, and M. Jendryke, "A preliminary investigation of Luojia-1 night-time light imagery," *Remote Sens. Lett.*, vol. 10, no. 6, pp. 526–535, 2019.

[13] Z. Yang, Y. Chen, G. Guo, Z. Zheng, and Z. Wu, "Using nighttime light data to identify the structure of polycentric cities and evaluate urban centers," *Sci. Total Environ.*, vol. 780, 2021, Art. no. 146586.

[14] X. Li, F. Duarte, and C. Ratti, "Analyzing the obstruction effects of obstacles on light pollution caused by street lighting system in Cambridge, Massachusetts," *Environ. Plan. B, Urban Analytics City Sci.*, vol. 48, no. 2, pp. 216–230, 2021.

[15] Y. Xu, Y. Song, J. Cai, and H. Zhu, "Population mapping in China with Tencent social user and remote sensing data," *Appl. Geogr.*, vol. 130, 2021, Art. no. 102450.

[16] P. Gong et al., "Mapping essential urban land use categories in China (EULUC-China): Preliminary results for 2018," *Sci. Bull.*, vol. 65, no. 3, pp. 182–187, 2020.

[17] Y. Ye et al., "A new perspective to map the supply and demand of artificial night light based on Loujia1-01 and urban big data," *J. Cleaner Prod.*, vol. 276, 2020, Art. no. 123244.

[18] H. Letu et al., "Estimating energy consumption from night-time DMPS/OLS imagery after correcting for saturation effects," *Int. J. Remote Sens.*, vol. 31, no. 16, pp. 4443–4458, 2010.

[19] H. Letu, M. Hara, G. Tana, and F. Nishio, "A saturated light correction method for DMSP/OLS nighttime satellite imagery," *IEEE Trans. Geosci. Remote Sens.*, vol. 50, no. 2, pp. 389–396, Feb. 2012.

[20] J. Wu, S. He, J. Peng, W. Li, and X. Zhong, "Intercalibration of DMSP-OLS night-time light data by the invariant region method," *Int. J. Remote Sens.*, vol. 34, no. 20, pp. 7356–7368, 2013.

[21] Z. Cao, Z. Wu, Y. Kuang, and N. Huang, "Correction of DMSP/OLS nighttime light images and its application in China," *J. Geo-Inf. Sci.*, vol. 17, no. 9, pp. 1092–1102, 2015.

[22] D. Lu, H. Tian, G. Zhou, and H. Ge, "Regional mapping of human settlements in southeastern China with multisensor remotely sensed data," *Remote Sens. Environ.*, vol. 112, no. 9, pp. 3668–3679, 2008.

[23] Q. Zhang, C. Schaaf, and K. C. Seto, "The vegetation adjusted NTL urban index: A new approach to reduce saturation and increase variation in nighttime luminosity," *Remote Sens. Environ.*, vol. 129, pp. 32–41, 2013.

[24] L. Zhuo, X. F. Zhang, J. Zheng, H. Y. Tao, and Y. B. Guo, "An EVI based method to reduce saturation of DMSP/OLS nighttime light data," *Acta Geographica Sin.*, vol. 70, no. 8, pp. 1339–1350, 2015.

[25] W. Guo, D. Lu, Y. Wu, and J. Zhang, "Mapping impervious surface distribution with integration of SNNP VIIRS-DNB and MODIS NDVI data," *Remote Sens.*, vol. 7, no. 9, pp. 12459–12477, 2015.

[26] Q. Zhang, B. Li, D. Thau, and R. Moore, "Building a better urban picture: Combining day and night remote sensing imagery," *Remote Sens.*, vol. 7, no. 9, pp. 11887–11913, 2015.

[27] X. Liu, G. Hu, B. Ai, X. Li, and Q. Shi, "A normalized urban areas composite index (NUACI) based on combination of DMSP-OLS and MODIS for mapping impervious surface area," *Remote Sens.*, vol. 7, no. 12, pp. 17168–17189, 2015.

[28] R. Hao, D. Yu, Y. Sun, Q. Cao, Y. Liu, and Y. Liu, "Integrating multiple source data to enhance variation and weaken the blooming effect of DMSP-OLS light," *Remote Sens.*, vol. 7, no. 2, pp. 1422–1440, 2015.

[29] X. Zhang and P. Li, "A temperature and vegetation adjusted NTL urban index for urban area mapping and analysis," *ISPRS J. Photogramm. Remote Sens.*, vol. 135, pp. 93–111, 2018.

[30] X. Chen, X. Jia, and M. Pickering, "A nighttime lights adjusted impervious surface index (NAISI) with integration of Landsat imagery and nighttime lights data from International Space Station," *Int. J. Appl. Earth Observ. Geo-Inf.*, vol. 83, 2019, Art. no. 101889.

[31] L. Ma, J. Wu, W. Li, J. Peng, and H. Liu, "Evaluating saturation correction methods for DMSP/OLS nighttime light data: A case study from China's cities," *Remote Sens.*, vol. 6, no. 10, pp. 9853–9872, 2014.

[32] Y. Liu, Y. Yang, W. Jing, L. Yao, X. Yue, and X. Zhao, "A new urban index for expressing inner-city patterns based on MODIS LST and EVI regulated DMSP/OLS NTL," *Remote Sens.*, vol. 9, no. 8, 2017, Art. no. 777.

[33] B. Wu, C. Yang, Q. Wu, C. Wang, J. Wu, and B. Yu, "A building volume adjusted nighttime light index for characterizing the relationship between urban population and nighttime light intensity," *Comput. Environ. Urban Syst.*, vol. 99, 2023, Art. no. 101911.

[34] X. Li, X. Yang, and L. Gong, "Evaluating the influencing factors of urbanization in the Xinjiang Uygur Autonomous Region over the past 27 years based on VIIRS-DNB and DMSP/OLS nightlight imageries," *PLOS One*, vol. 15, no. 7, 2020, Art. no. e0235903.

[35] Y. Zhou, X. Li, and Y. Liu, "Cultivated land protection and rational use in China," *Land Use Policy*, vol. 106, no. 1, 2021, Art. no. 105454.

[36] Y. Ou, L. Tang, X. Wei, and Y. Li, "Spatial interaction between urbanization and ecosystem services in Chinese urban agglomerations," *Land Use Policy*, vol. 109, no. 4, 2021, Art. no. 105587.

[37] C. Fang, Q. Gao, X. Zhang, and W. Cheng, "Spatiotemporal characteristics of the expansion of an urban agglomeration and its effect on the eco-environment: Case study on the northern slope of the Tianshan Mountains," *Sci. China Earth Sci.*, vol. 62, no. 9, pp. 1461–1472, 2019.

[38] R. Wu, D. Yang, J. Dong, L. Zhang, and F. Xia, "Regional inequality in China based on NPP-VIIRS night-time light imagery," *Remote Sens.*, vol. 10, no. 2, 2018, Art. no. 240.

[39] B. N. Holben, "Characteristics of maximum-value composite images from temporal AVHRR data," *Int. J. Remote Sens.*, vol. 7, no. 11, pp. 1417–1434, 1986.

[40] T. Graichen, J. Richter, R. Schmidt, and U. Heinkel, "Improved indoor positioning by means of occupancy grid maps automatically generated from OSM indoor data," *ISPRS Int. J. Geo-Inf.*, vol. 10, no. 4, 2021, Art. no. 216.

[41] X. Cao, J. Chen, H. Imura, and O. Higashi, "A SVM-based method to extract urban areas from DMSP-OLS and SPOT VGT data," *Remote Sens. Environ.*, vol. 113, no. 10, pp. 2205–2209, 2009.

[42] M. Hara, S. Okada, H. Yagi, T. Moriyama, K. Shigehara, and Y. Sugimori, "Progress for stable artificial lights distribution extraction accuracy and estimation of electric power consumption by means of DMSP/OLS night-time imagery," *Int. J. Remote Sens. Earth Sci.*, vol. 1, no. 1, pp. 31–42, 2010.

[43] Z. Zheng, Y. Chen, Z. Wu, and Q. Zhang, "Method to reduce saturation of DMSP/OLS nighttime light data based on UNL," *J. Remote Sens.*, vol. 22, no. 1, pp. 161–173, 2018.

[44] N. Levin et al., "Remote sensing of night lights: A review and an outlook for the future," *Remote Sens. Environ.*, vol. 237, 2020, Art. no. 111443.

Haofan Ran received the B.S. degree in geographic information science from Xinjiang University, Urumqi, China, in 2021. He is currently working toward the M.S. degree in resources and environment with the University of Chinese Academy of Sciences, Beijing, China.

His research interests include remote sensing research on city and air environment, remote sensing image classification, urbanization dynamic detection, and image processing.

Fei Zhang received the M.S. degree in cartography and geography information system and Ph.D. degree in ecology from Xinjiang University, Urumqi, China, in 2007 and 2011, respectively.

He is currently a Professor with the College of Geography and Environmental Sciences, Zhejiang Normal University, Jinhua, China. His research interests include remote sensing research on water environment, remote sensing image classification, urbanization dynamic detection, and image processing.

Ngai Weng Chan received the M.S. degree in climatology and meteorology from the University of Malaya, Kuala Lumpur, Malaysia, in 1977, and the Ph.D. degree in environmental hazards management (floods) from Middlesex University, London, U.K., in 1995.

He is currently a Professor with GeoInformatic Unit, Geography Section, School of Humanities, Universiti Sains Malaysia, Penang, Malaysia. His research interests include hydroclimatology, water resources, and hazards management.

Mou Leong Tan received the B.Sc. and Ph.D. degrees in remote sensing from the Universiti Teknologi Malaysia, Johor Bahru, Malaysia, in 2012 and 2016, respectively.

In 2017, he completed his Postdoctoral Fellowship with the National University of Singapore. He is currently a Senior Lecturer with the GeoInformatic Unit, Geography Section, School of Humanities, Universiti Sains Malaysia, Penang, Malaysia. He is also the Vice President of Water Watch Penang. His research interests include remote sensing and GIS research on climate change, hydrology, solar energy, solar geoengineering, satellite data reliability assessment, etc.

Hsiang-Te Kung received the M.S. and Ph.D. degrees in geography and geology from the University of Tennessee, Knoxville, TN, USA, in 1972 and 1980, respectively.

He is currently a Professor with the Department of Earth Sciences, University of Memphis, Memphis, TN, USA His research interests include water resources, hydrologic process, water balance, and watershed management.

Jingchao Shi received the B.S. degree in electronic information engineering from Xinjiang University, Urumqi, China, in 2007, and the M.S. degree in accounting and economics from Florida Atlantic University, Boca Raton, FL, USA, in 2019. He is currently working toward the Ph.D. degree in earth sciences with the University of Memphis, Memphis, TN, USA.

His research interests include future climate change, climate change impact on water resources, and flooding frequency and management.